SUPPLEMENTAL MATERIALS AND METHODS

atpD knockout and complementation

One copy of *atpD* gene in *M. smegmatis* mc^{2}155 was replaced with the hygromycin cassette (*hyg*^{R}) by following the method described elsewhere (3, 12). Briefly, hygromycin cassette was PCR amplified from pVV16 plasmid (BEI resources), and was sandwiched between 600 bp upstream and downstream DNA fragments of *atpD* gene that were PCR amplified from *M. smegmatis* genomic DNA. The allelic exchange substrate (AES) thus generated was used to replace one copy of *atpD* gene. Knockout was confirmed by PCR using oligos specific for the gene sequence, followed by DNA sequencing of the amplified fragment. For complementation, the full length *atpD* gene was PCR amplified using Msm mc^{2}155 genomic DNA as template and was cloned into pMVAcet (10) between NdeI and EcoRI sites. The plasmid (pMVAcet-*atpD*) was electroporated in the wild-type and the *atpD*-deleted *M. smegmatis* cells and the transformants were selected on MB7H9-agar plates supplemented with kanamycin.

Protein expression analysis

To assess the expression of AtpD levels in *M. smegmatis* WT and Δ*atpD*, the bacterial cells were harvested by centrifugation at room temperature, resuspended in lysis buffer containing 8 M urea in 1X phosphate-buffered saline (PBS), and lysed by sonication. The lysate was centrifuged at high speed for 10 min at RT. Supernatant was collected, and the protein concentration in it was determined using Bradford assay. The supernatant was mixed with SDS loading buffer, boiled for 5 min, and loaded on a 12% SDS polyacrylamide gel. The separated proteins were then transferred onto a polyvinylidene difluoride (PVDF) membrane (Millipore), and Western

blotting was carried out using anti-AtpD antibody raised in rabbit, followed by anti-rabbit IgG DyLight 800-conjugated secondary antibody (Thermo). RpoB protein as probed with RNA polymerase anti-RpoB antibodies (Thermo) was used as loading control. The blots were imaged on an Odyssey infrared imaging system (LI-COR Biosciences, Lincoln, NE).

Kill kinetics assay

Bedaquiline (HY-14881) was obtained from MedChemExpress, USA. Stock solutions of drug compound were prepared by reconstitution in DMSO. All other antibiotics, as mentioned, were obtained from Sigma Aldrich. To monitor the kill kinetics assay, bacterial cultures were adjusted to OD600 ~0.6, and BDQ was added to a final concentration of 0.0001 $\mu g\,ml^{-1}$, wherever required. For antibiotic-mediated killing, concentrations as specified were added in the culture medium. At indicated time points, samples were taken and OD600 was recorded. The values were then obtained to generate kill kinetics plot.

Congo red dye assay

Log phase bacterial culture (OD_{600} ~1) was centrifuged at 5000 × g for 20 min at RT. The pellet was subsequently re-suspended in 1X-PBST buffer (0.137 M NaCl, 0.0027 M KCl, 0.01 M Na_2HPO_4, 0.0018 M KH_2PO_4, 0.05% tween 80). 2 µl of cell suspension (OD_{600} ~1) was spotted on 100 µg/ml Congo red dye-containing MB7H9-agar plate. The plates were incubated for 3 days at 37°C, and the colonies were imaged (11, 13).

Peroxide stress assay

Sensitivity of *M. smegmatis* to H_2O_2 was examined by spot assay and zone inhibition assay. Briefly, *M. smegmatis* log phase cultures (OD_{600} ~0.6) were treated with H_2O_2 at the indicated concentrations for a period of 6 h. The cultures were harvested at indicated time points and washed with 1X-PBST. The cells were resuspended in 1X-PBST and various dilutions ($10^0 – 10^{-4}$) were spotted on MB7H9 agar plates supplemented with 2% glucose. The plates were incubated at 37°C for 48 h and imaged. For peroxide stress rescue experiment, the log phase culture (OD_{600} ~0.6) was treated with 20 mM H_2O_2 along with either 10 mM 4HT or 150 mM thiourea for 12 h. The culture was subsequently spotted on agar plate. The plates were incubated and imaged as described above. For zone inhibition assay, 5 mM H_2O_2 was spotted at the centre of MB7H9 soft agar plate (MB7H9 broth supplemented with 0.3% agarose) containing *M. smegmatis* culture of respective strains. The plates were incubated at 37°C for 48 h. The plates were imaged and the diameter of the zone of growth inhibition was measured.

GPL extraction and analysis by thin layer chromatography and mass spectrometry

Glycopeptidolipids (GPL) were extracted as described previously (11) with some modifications. Briefly, log phase culture (50 ml, OD_{600} ~2) grown in MB7H9 broth supplemented with 2% glucose and 0.05% tween-80was harvested by centrifugation at 5000 × g for 20 min at RT, and the cell pellet was washed with 10 ml of phosphate buffered saline (PBS). GPLs were extracted by treating the cells with 2:1 (v/v) ratio of $CHCl_3$ and CH_3OH (20 µl/mg wet weight) and incubating overnight at RT in shaking condition. The supernatant was recovered by centrifugation (18,000 × g, 15 min, RT) and mixed with 0.2 volumes of 0.9% NaCl followed by

vortexing vigorously. The mixture was further centrifuged (1000 × g, 10 min, RT) and the organic phase containing GPLs was recovered and dried. The dried lipids were then dissolved in 50 µl of $CHCl_3$/CH_3OH (2:1 v/v) and were subjected to TLC on an aluminum-backed silica gel plates. TLCs were developed in $CHCl_3$/CH_3OH (100:7 v/v). The plates were allowed to dry, and were sprayed with orcinol/sulfuric acid (0.1% orcinol v/v in 40% sulfuric acid in water). GPLs were detected by charring at 140°C until the color developed. For mass spectrometric analysis, lipids were extracted from the unstained TLC, and were subjected to electrospray ionization quadrupole time-of-flight (Q-ToF) mass spectrometer (Bruker). Total ion chromatogram (TIC) was obtained, and was analyzed.

Polar and apolar lipid extraction and analysis by thin layer chromatography and mass spectrometry

Polar and apolar lipids were extracted following the previously described protocol (1, 4). Briefly, mycobacterial log phase culture grown in MB7H9 broth supplemented with 2% glucose and 0.05% tween 80 was harvested and 300 mg of lyophilized cells with equal weight (obtained from log phase culture of the desired bacterium) were suspended in methanolic saline containing methanol:0.3% NaCl (100:10) mixed with petroleum ether and rotated for 20 min. The extract was centrifuged at 4500 × g for 20 min at RT. The upper petroleum ether layer was recovered carefully and the pellet was extracted again with 2 ml of petroleum ether. Both petroleum ether extracts were then combined and evaporated under nitrogen to yield apolar lipids, which were further resuspended in dichloromethane before thin layer chromatography (TLC) analysis. Equal amounts of apolar lipids were then loaded on TLC and separated by developing TLC in

hexane:ethyl acetate (90:10) and visualized by charring. For extraction of polar lipids, the methanolic saline extract was heated in a boiling-water bath for 10 min, allowed to cool to RT, and then mixed with 3 ml of chloroform:methanol:0.3% NaCl (9:10:3), and rotated for 1 h at RT. The biomass was recovered and further extracted by adding 0.75 ml of chloroform:methanol:0.3% NaCl (5:10:4) and centrifuging at 3200 × g for 30 min at RT. Both the solvent extracts were combined, mixed with 2 ml of chloroform and 2 ml of 0.3% NaCl, rotated for 30 min, and were subsequently centrifuged at 2600 × g at RT to separate the lower organic and the upper aqueous phases. The aqueous phase was discarded, and the organic phase was dried to yield polar lipids. The dried lipids were then dissolved in chloroform:methanol (2:1) prior to TLC analysis. Equal amount of polar lipids were then loaded on TLC and were further separated by developing TLC in chloroform:methanol:water (60:30:6) and visualized by charring at 120°C after staining with iodine vapours. Apolar lipids were visualized by spraying with 5% ethanolic-phosphomolybdic acid, and charring as described above. For mass spectrometric analysis, lipids were extracted from the unstained TLC, and were subjected to electrospray ionization quadrupole time-of-flight (Q-ToF) mass spectrometer (Bruker). Total ion chromatogram (TIC) was obtained, and was analyzed.

Sensitivity towards SDS, pH, lysozyme, and antibiotics

Log phase cultures (OD_{600} ~0.6) of bacteria were harvested and washed with 1X-PBST. To measure the sensitivity towards acidic pH, bacterial cells were grown in MB7H9 medium having pH 5.5 for 24 h at 37°C, and spotted on an MB7H9-agar plate. Sensitivity towards SDS and lysozyme was assessed by growing the cells in the presence of either 0.1% SDS or lysozyme (25

μg/ml, 250 μg/ml) for specified time points at 37°C, and spotting them on an MB7H9-agar plate. The cells were also treated with different antibiotics such as tetracycline (3 μg/ml), chloramphenicol (32 μg/ml), vancomycin (5 μg/ml), rifampicin (20 μg/ml), isoniazid (20 μg/ml), streptomycin (4 μg/ml), and triclosan (30 μg/ml) for different time points as specified, and spotted. In each case, before spotting, the cultures were harvested at indicated time points, washed with 1X-PBST, and various dilutions (10^0 to 10^{-4}) were spotted on an MB7H9-agar plate. The plates were then incubated and imaged.

Transmission electron microscopy (TEM)

Transmission electron microscopy was carried as described previously (6) with some modifications. *M. smegmatis* cells were fixed in 0.15 M sodium cacodylate buffer containing 1% osmium tetraoxide for 1 h at RT. The cells were then washed with cacodylate buffer followed by post fixation for 2 h at RT in 0.15 M sodium cacodylate buffer containing 2% tannic acid and 2% glutaraldehyde solution. The cells were then again washed with cacodylate buffer and re-fixed in 1% osmium tetraoxide overnight at 4°C. Samples were then washed with MilliQ water and embedded in 2% molten agarose. The agar blocks were cut into very fine pieces and were subjected to sequential acetone dehydration at increasing concentrations for 30 min each (30%, 50%, 70%, 90%, and 100%). Samples were infiltrated overnight with Spurr's resin and acetone in equal volume at RT. The infiltrated samples containing Spurr's resin were embedded in mold and allowed to set at 70°C for 48 h. Ultrathin sections were then cut on microtome and picked up on a copper grid. The grids were further stained with 1% uranyl acetate followed by 0.1%

phosphotungstic acid, and imaged on FEI Talos 200S system, equipped with a 200kV Field Emission Gun.

Scanning electron microscopy (SEM)

For scanning electron microscopy, the procedure was adapted as described previously (5, 8) with some modifications. Briefly, the log phase cultures were harvested by centrifugation. The bacterial pellets were washed in MB7H9 broth twice and were fixed overnight in 0.1 M sodium cacodylate buffer containing 2% paraformaldehyde and 2.5% glutaraldehyde, at 4°C. The cells were then harvested and washed with 0.1 M sodium cacodylate buffer followed by fixing the cells with 2% osmium tetraoxide in MilliQ water for 2 h at RT. Cells were then washed with 0.1 M sodium cacodylate buffer followed by sequential dehydration through a series of graded ethanol (20%, 50%, 70%, 90%, 100%) for 15 min, and dried by vacuum desiccation. The samples were then attached to stubs, sputter-coated with gold, and imaged on UltraPlus scanning electron microscope (ZEISS, Germany) at 10.0 kV.

Cell viability assay

Cell viability assays were performed using a fluorescent dye indicator alamarBlue (Thermo), by following the method as described previously (9), with some modifications. Briefly, log phase culture cells (OD_{600} ~0.6) were harvested, washed with 1X-PBST, and resuspended in the same buffer. 180 µl of cell suspension along with 10% alamarBlue was added to each well of a 96-well plate. alamarBlue is a redox-sensitive dye. Upon entering the cells, resazurin (7-hydroxy-3H-

phenoxazin-3-one10-oxide), which is the active dye component, is reduced to resorufin leading to increased fluorescence, thus suggesting the presence of viable cells. Intensity of fluorescence is directly proportional to the number of viable cells present. Plates were incubated in dark at 37°C for 3 h on a thermomixer. Fluorescence was recorded by using the Ex/Em of 530/590 nm on SpectraMax M5 plate reader.

ROS estimation

ROS production was measured using ROS sensing dye DCHFDA (2'-7'-dichlorodihydrofluorescein diacetate; Sigma) with Ex/Em of 495/530 nm. The protocol was adapted as described previously (2, 7). Briefly, log phase culture of OD_{600} ~0.6 was harvested and washed with 1X-PBST. 200 µl of cell suspension was added to 96-well plates to which DCHFDA dye was added to a final concentration of 10 µM. Plates were incubated in dark at 25°C for 1 h on a thermomixer. Fluorescence was recorded on SpectraMax M5 plate reader.

Oxygen consumption

Respiration rate via oxygen consumption was measured on a Clark-type oxygen electrode (Hansatech). The electrode was fully aerated (250 µM O_2 at 25°C) and calibrated with sodium dithionite. Log phase cultures of bacterial strains (OD_{600} ~1) were used. Cultures were centrifuged for 5 min at 6000 × g at 4°C, washed and re-suspended again in MB7H9 medium. 2 ml of culture was then added to the incubation chamber and the basal oxygen consumption was monitored for 10 min. When required, the ETC inhibitor (rotenone or antimycin A) at a final

concentration of 0.5 μM was added and the measurement was continued. Values obtained were used to plot the %oxygen saturation graph.

RNA extraction, cDNA synthesis, and RT-qPCR

Differential gene expression profile was obtained by reverse transcription-quantitative PCR (RT-qPCR) for bacteria as described previously (3). Briefly, cells were grown till OD ~ 0.8. The cultures were then harvested and the RNA was isolated using TRI Reagent (Sigma-Aldrich). cDNA was synthesized using i-script cDNA synthesis kit (Bio-Rad) following the manufacturer's instructions. The cDNA so obtained was further used for qPCR. *rpoB* gene was used as an internal control. qPCR was carried out on a StepOnePlus real-time PCR system (Applied Biosystems) using iTaq universal SYBR green mix (Bio-Rad) as per the manufacturer's instructions. RT-qPCR reactions were performed and the data were analysed as per $2^{-\Delta\Delta Ct}$ method as described (3). Sequences of the oligos used for qPCR are listed in table S1.

References

1. Billman-Jacobe, H., M. J. McConville, R. E. Haites, S. Kovacevic, and R. L. Coppel. 1999. Identification of a peptide synthetase involved in the biosynthesis of glycopeptidolipids of *Mycobacterium smegmatis*. Mol Microbiol 33:1244-1253.
2. Borisov, V. B., E. Forte, A. Davletshin, D. Mastronicola, P. Sarti, and A. Giuffre. 2013. Cytochrome bd oxidase from *Escherichia coli* displays high catalase activity: an additional defense against oxidative stress. FEBS Lett 587:2214-2218.
3. Dubey, A. A., S. R. Wani, and V. Jain. 2018. Methylotrophy in mycobacteria: Dissection of the methanol metabolism pathway in *Mycobacterium smegmatis*. J Bacteriol 200:e00288-00218.
4. Folch, J., M. Lees, and G. H. Sloane Stanley. 1957. A simple method for the isolation and purification of total lipides from animal tissues. J Biol Chem 226:497-509.
5. Gupta, K. R., P. Baloni, S. S. Indi, and D. Chatterji. 2016. Regulation of Growth, Cell Shape, Cell Division, and Gene Expression by Second Messengers (p)ppGpp and Cyclic Di-GMP in *Mycobacterium smegmatis*. J Bacteriol 198:1414-1422.
6. Gupta, K. R., S. Kasetty, and D. Chatterji. 2015. Novel functions of (p)ppGpp and Cyclic di-GMP in mycobacterial physiology revealed by phenotype microarray analysis of wild-type and isogenic strains of *Mycobacterium smegmatis*. Appl Environ Microbiol 81:2571-2578.
7. Howell Wescott, H. A., D. M. Roberts, C. L. Allebach, R. Kokoczka, and T. Parish. 2017. Imidazoles Induce Reactive Oxygen Species in *Mycobacterium tuberculosis* Which Is Not Associated with Cell Death. ACS Omega 2:41-51.
8. Li, Q. M., M. L. Zhou, X. Y. Fan, J. L. Yan, W. M. Li, and J. P. Xie. 2016. Mycobacteriophage SWU1 gp39 can potentiate multiple antibiotics against *Mycobacterium* via altering the cell wall permeability. Sci Rep 6:28701.
9. O'Brien, J., I. Wilson, T. Orton, and F. Pognan. 2000. Investigation of the Alamar Blue (resazurin) fluorescent dye for the assessment of mammalian cell cytotoxicity. Eur J Biochem 267:5421-5426.
10. Pohane, A. A., H. Joshi, and V. Jain. 2014. Molecular dissection of phage endolysin: an interdomain interaction confers host specificity in Lysin A of *Mycobacterium* phage D29. J Biol Chem 289:12085-12095.
11. Tatham, E., S. Sundaram Chavadi, P. Mohandas, U. R. Edupuganti, S. K. Angala, D. Chatterjee, and L. E. Quadri. 2012. Production of mycobacterial cell wall glycopeptidolipids requires a member of the MbtH-like protein family. BMC Microbiol 12:118.
12. van Kessel, J. C., L. J. Marinelli, and G. F. Hatfull. 2008. Recombineering mycobacteria and their phages. Nat Rev Microbiol 6:851-857.
13. Zanfardino, A., A. Migliardi, D. D'Alonzo, A. Lombardi, M. Varcamonti, and A. Cordone. 2016. Inactivation of MSMEG_0412 gene drastically affects surface related properties of *Mycobacterium smegmatis*. BMC Microbiol 16:267.

SUPPLEMENTAL FIGURES

Figure S1

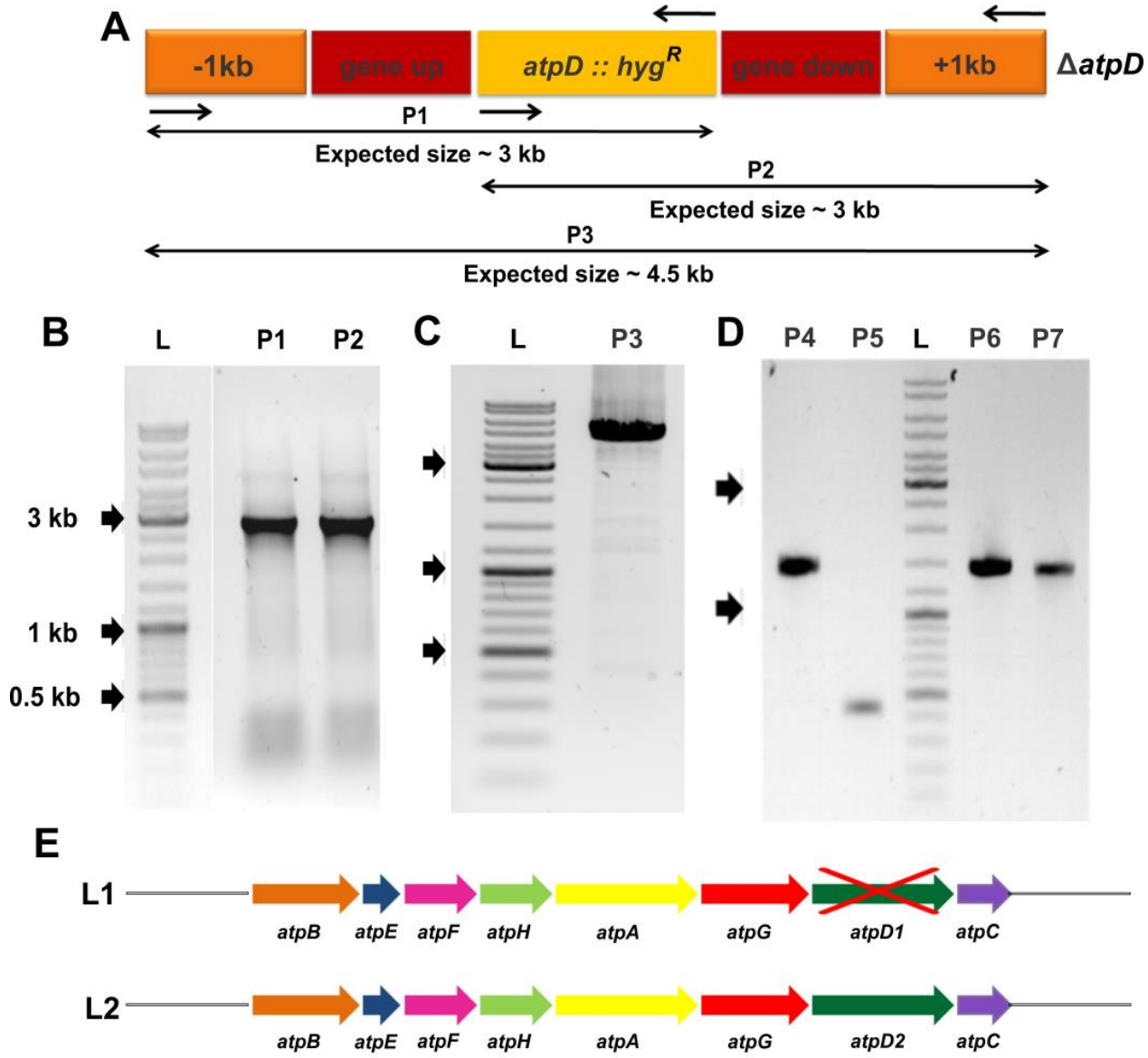

Figure 1. Confirmation of *M. smegmatis atpD* knockout. (A) Cartoon representation of the replacement of only one copy of *atpD* gene (1428 bp) with hygromycin cassette (hyg^R) (1382 bp) in *M. smegmatis* is provided. Various oligos (shown as short arrows) used to confirm the knockout along with the expected product sizes after PCR are shown. The oligos along with their

sequences are given in table S1. **(B)** Agarose gel electrophoresis showing the PCR-amplified DNA bands of expected sizes that confirm *atpD* deletion. P1 and P2 are the amplified DNA bands produced using a set of primers (P1 = hyg_frw and ko_rev; P2 = ko_frw and hyg_rev) and *atpD* knockout bacterial genomic DNA as template. Both P1 and P2 correspond to the desired ~3kb amplification confirming the replacement of *atpD* gene by the correct insertion of hyg^R. **(C)** Agarose gel image shows the PCR amplification of complete ~4.5 kb region, as marked in panel A. The DNA was amplified using the primers ko_frw and ko_rev, and *atpD* knockout genomic DNA as template. (D) Agarose gel electrophoresis showing the PCR-amplified DNA bands using WT and *atpD* knockout genomic DNA as templates. P4-P7 are the amplified DNA bands produced using a set of primers (P4 and P6 = atpD_synβ_frw and atpD_synβ_rev) and (P5 and P7 = Hyg_frw and Hyg_rev). PCR amplification of 1.42 kb (P4) corresponds to the *atpD* gene in the WT, while an absence of amplification of 1.38 kb (P5) with the hygromycin primer set confirms the absence of hygromycin gene in the WT. Additionally, amplification of 1.42 kb (P6) corresponds to the second copy of the *atpD* gene in the knockout strain, confirming the presence of another intact copy, and the amplification of 1.38 kb (P7) with the hygromycin primer set further confirms the presence of hygromycin gene in the knockout strain. In panels B, C, and D, 'L' represents the DNA ladder with a few bands marked. **(E)** Schematic representation of the ATP synthase operon with all the genes marked in *M. smegmatis* is given. L1 and L2 represent the two loci, wherein one of the two copies of *atpD* gene in the operon is shown deleted, as verified by the PCR data from panels B, C, and D.

Figure S2

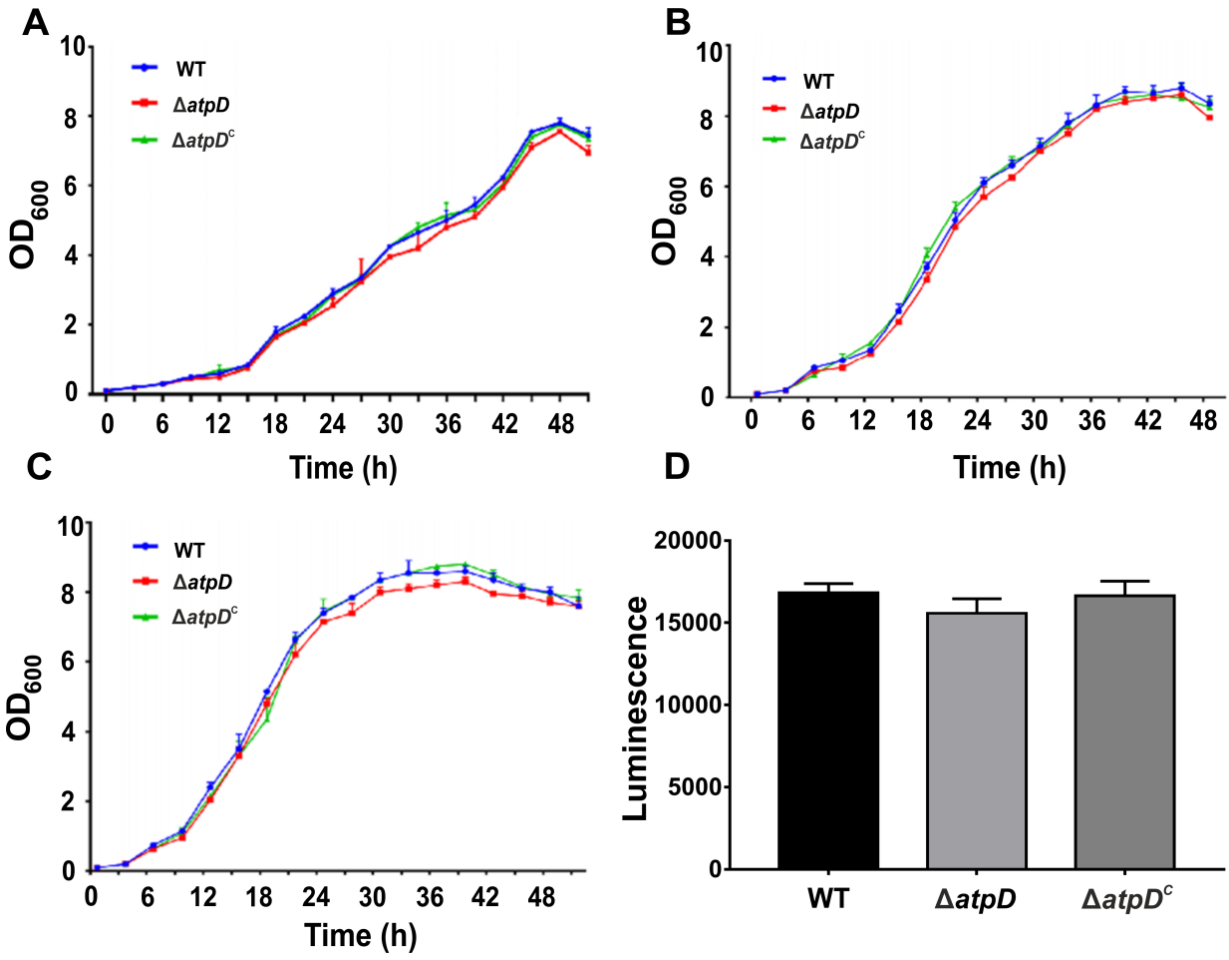

Figure S2. Growth analysis in LBT medium. Panels show the growth profiles of WT, Δ*atpD*, and Δ*atpD*^{C} strains at 28°C (A), 37°C (B), and 42°C (C) in LB broth supplemented with 0.05% tween 80 and 20mM glucose (LBT medium). The growth was monitored by measuring the optical density of the culture at 600 nm (OD_{600}) with time. Panel D represents the intracellular ATP estimation in WT, Δ*atpD*, and Δ*atpD*^{C} strains in LBT medium. Measured luminescence is plotted for all the three bacteria. No significant change in the luminescence is observed in all the three strains. Each plot in the graph is a representation of at least three independent experiments with standard deviation.

Figure S3

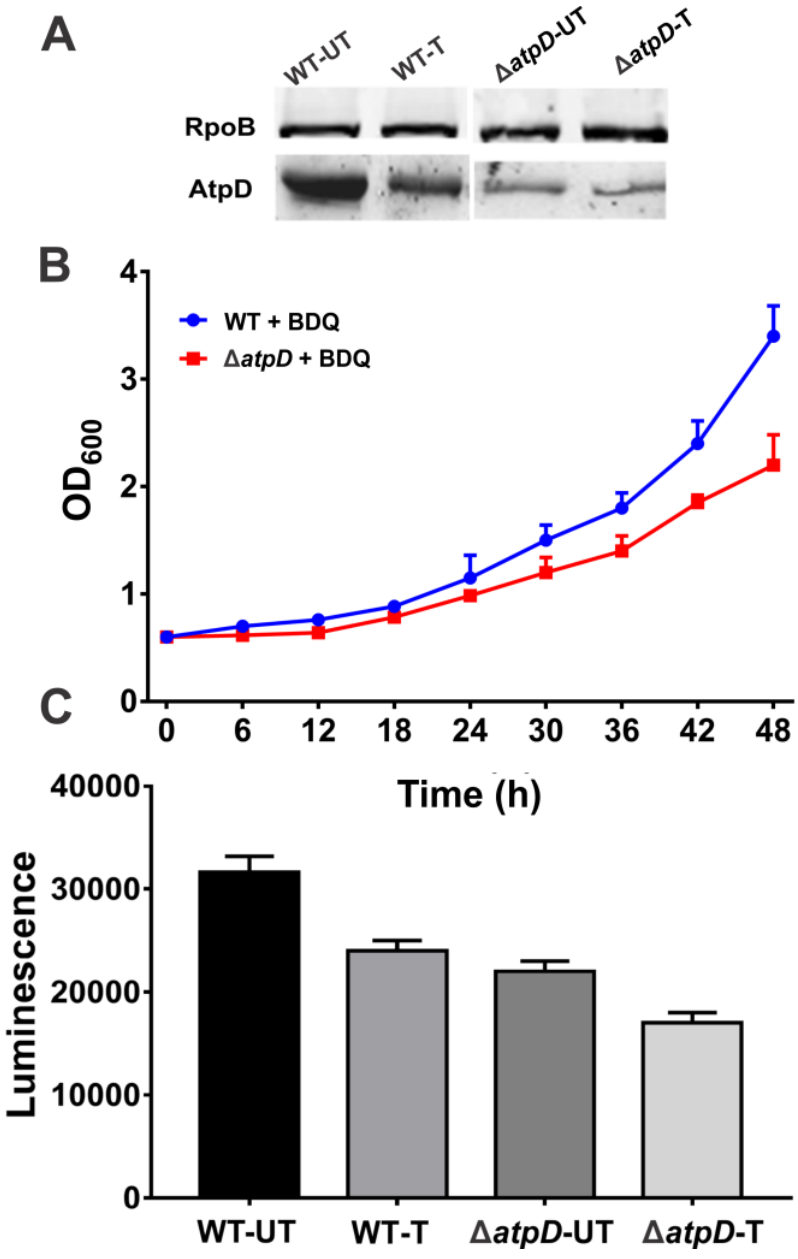

Figure S3. Effect of bedaquiline treatment on wild-type and *atpD* knockout. Panel A shows the Western blot of the whole cell lysate of bedaquiline-treated (T) or untreated (UT) wild-type (WT) and Δ*atpD* strain, probed with anti-AtpD and RNA polymerase anti-RpoB antibodies. The experiment was repeated at least thrice; only one representative image is shown. (B) Plot shows

the growth of bedaquiline-treated WT and Δ*atpD* strain in MB7H9 broth supplemented with 2% glucose as carbon source at 37°C. Growth was monitored as optical density of the culture at 600 nm (OD_{600}) with time and plotted. (C) Plot shows the intracellular ATP level in the bedaquiline-treated (T) or untreated (UT) wild-type (WT) and Δ*atpD* strain. Lower luminescence indicates low ATP level. In both panels B and C, data are an average of at least three independent experiments with standard deviation depicted as error bars.

Figure S4

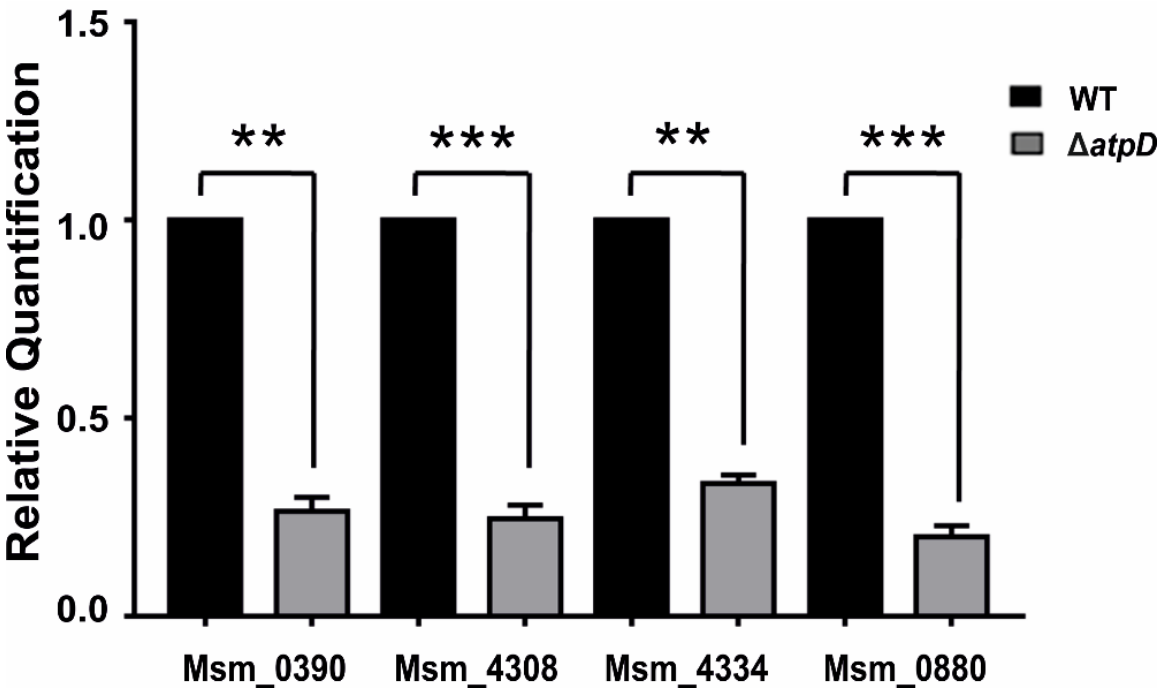

Figure S4. Expression analysis of genes involved in biofilm formation. RT-qPCR validation of differentially expressed genes involved in biofilm formation is shown. The total RNA was obtained from independent experiments performed under same biological conditions. The data indicate fold change in the expression of genes in *M. smegmatis* Δ*atpD* compared to the wild-type control. The error bar represents the standard deviation. Asterisk represents *P*-value; '**', ≤0.01; '***', ≤0.005.

Figure S5

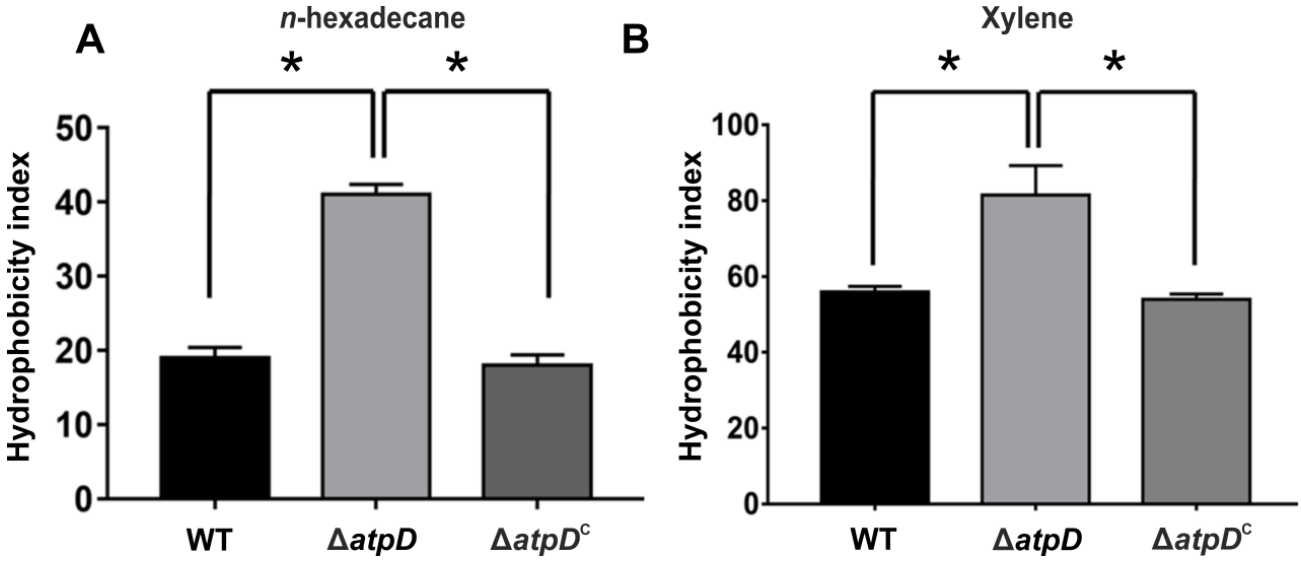

Figure S5. Hydrophobicity index in WT, Δ*atpD*, and Δ*atpD*^{C} strains. Hydrophobicity index as exhibited by WT, Δ*atpD*, and Δ*atpD*^{C} based on the degree of adherence to the two hydrocarbons viz. *n*-hexadecane (panel A) and xylene (panel B) is shown. In both cases, the mutant shows higher hydrophobicity compared to the other bacteria. '*' represents *P*-value <0.05.

Figure S6

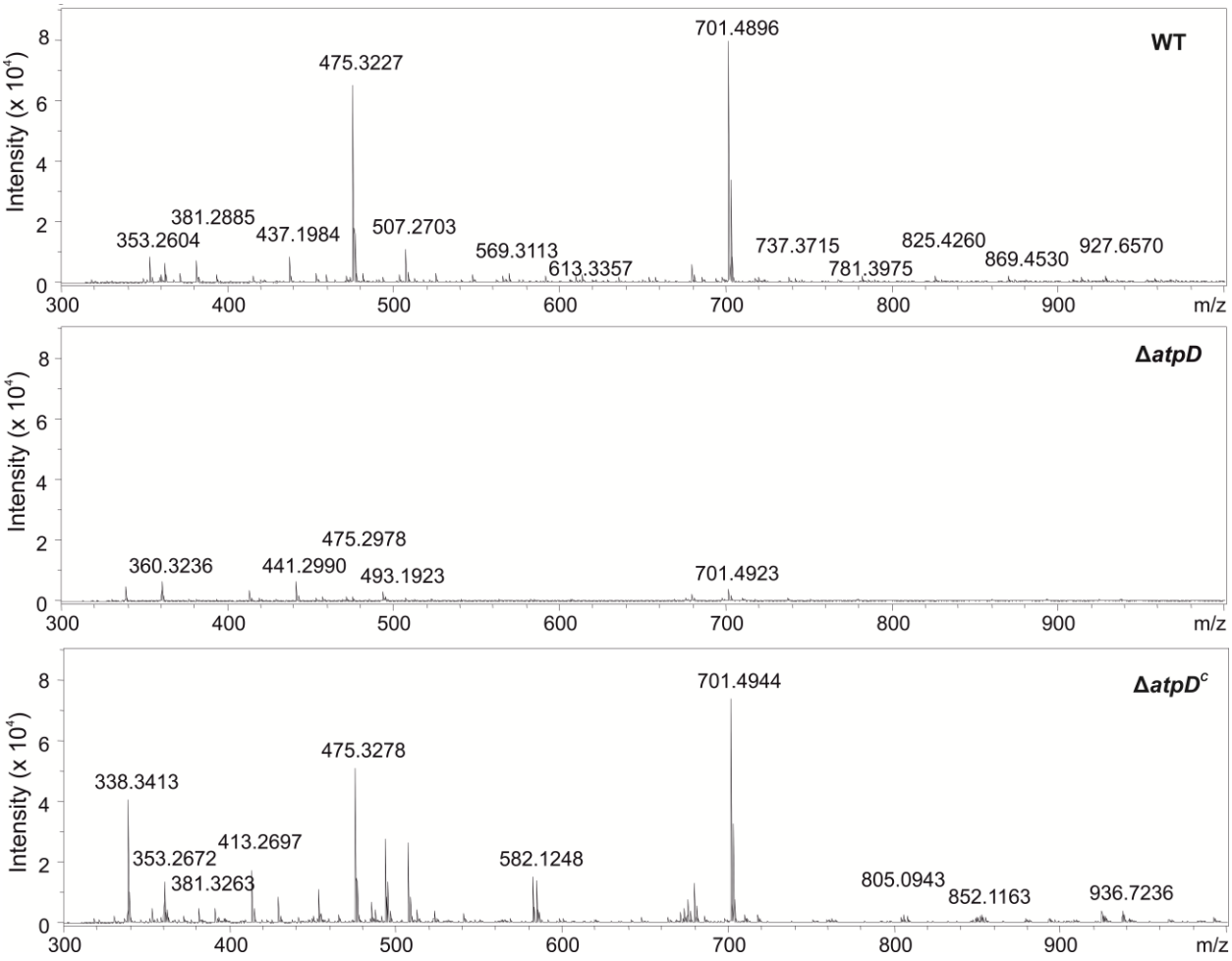

Figure S6. ESI-MS profiles of the Glycopeptidolipids (GPL). The panels show the comparison of complete ESI-MS spectra of GPLs isolated from WT, Δ*atpD*, and *atpD*^{C} strains. Some of the peaks are marked in each case. The mutant shows clear difference in several peaks such as 353.26 *m/z*, 381.29 *m/z*, 475.32 *m/z*, and 701.48 *m/z* as compared to those obtained in wild-type and the complemented strain.

Figure S7

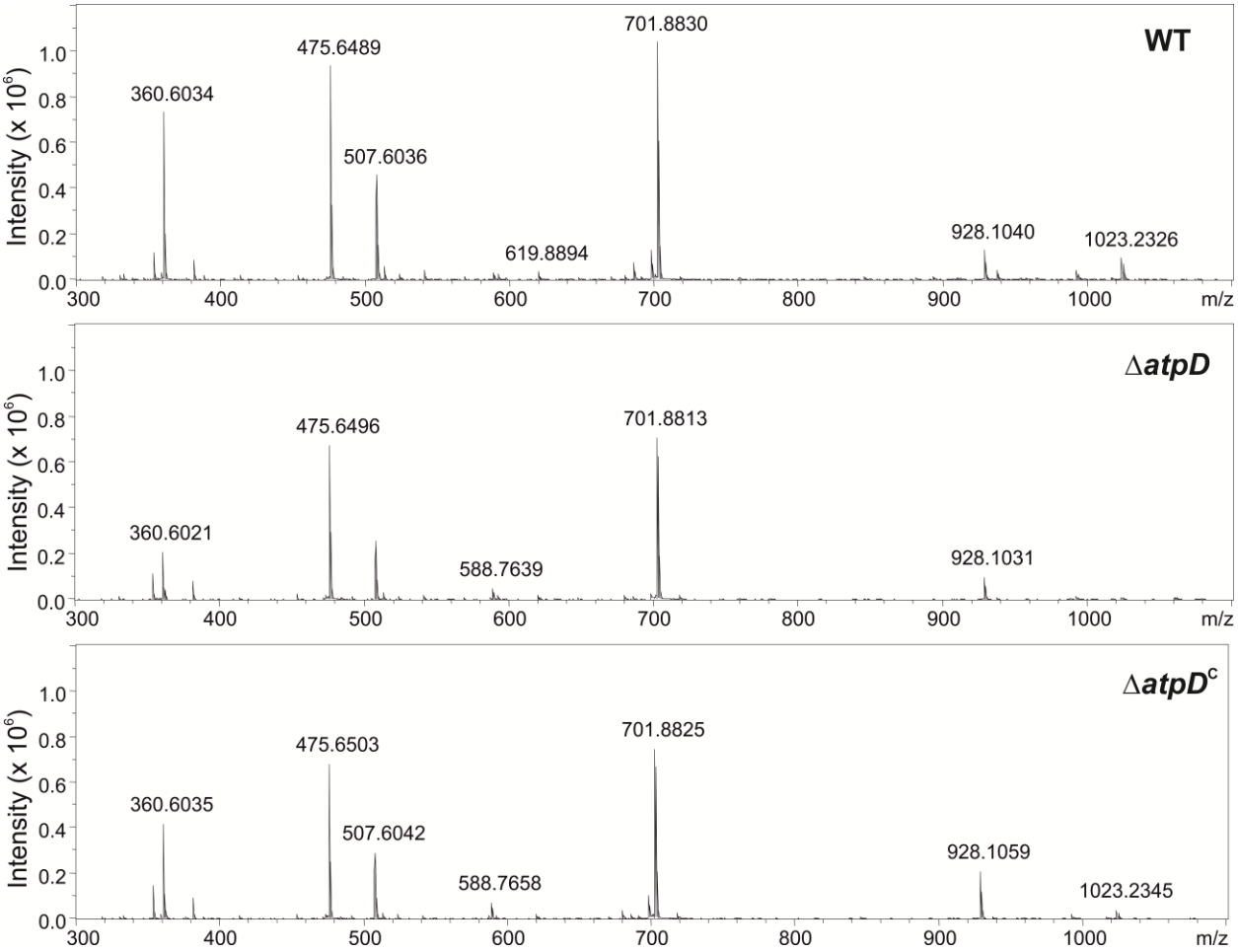

Figure S7. ESI-MS profiles of the polar lipids. The panels show the comparison of complete ESI-MS spectra of polar lipids isolated from WT, Δ*atpD*, and *atpD*^{C} strains. Some of the peaks are marked in each case. The mutant shows clear difference in several peaks such as 360.60 *m/z*, 507.60 *m/z*, and 928.10 *m/z* as compared to those obtained in wild-type and the complemented strain.

Figure S8

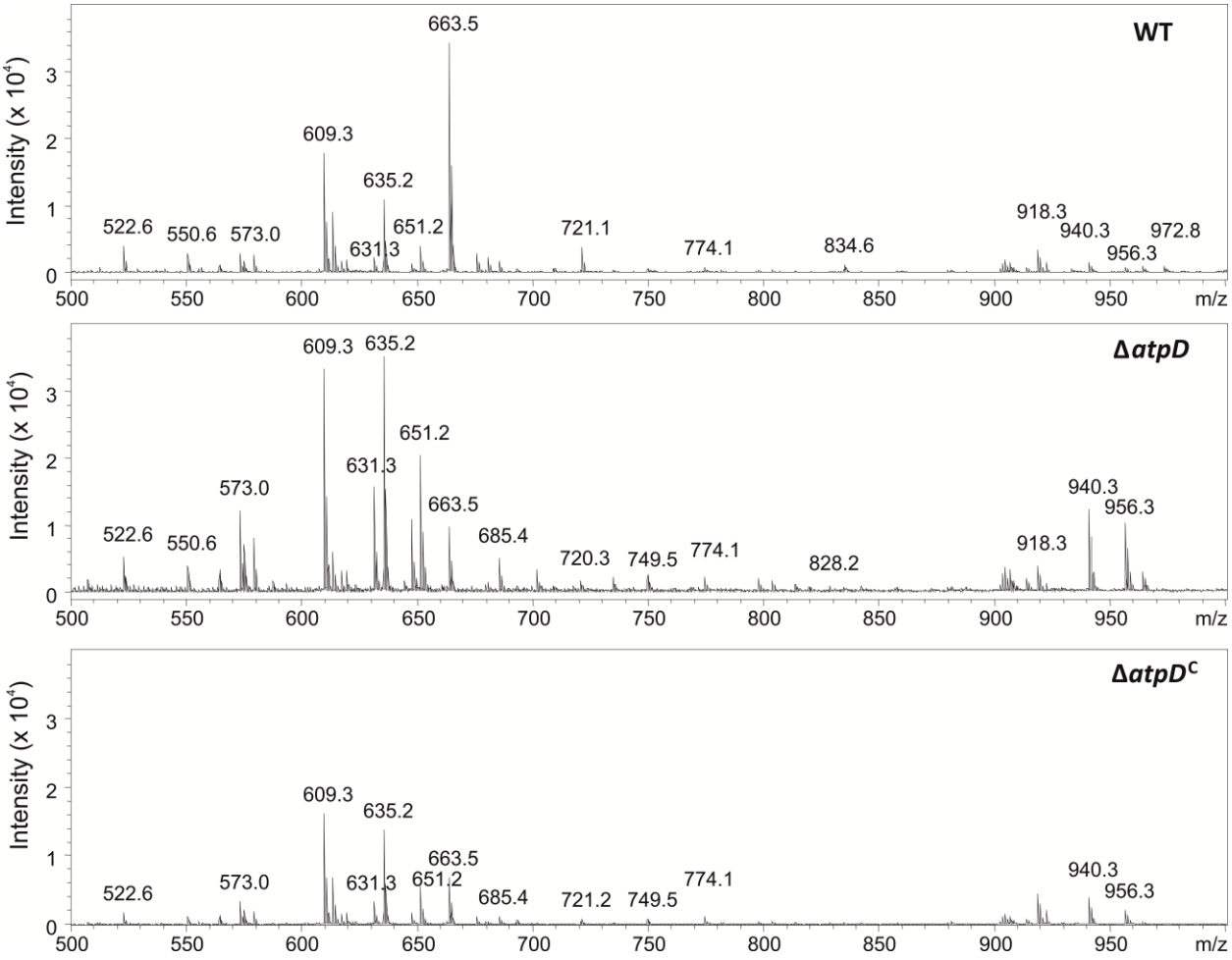

Figure S8. ESI-MS profiles of the apolar lipids. The panels show the comparison of complete ESI-MS spectra of apolar lipids isolated from WT, Δ*atpD*, and *atpD*^{C} strains. Some of the peaks are marked in each case. The mutant shows clear difference in several peaks such as 573.0 *m/z*, 609.3 *m/z*, 631.3 *m/z*, 635.2 *m/z*, 651.2 *m/z*, 940.3 *m/z*, and 956.3 *m/z* as compared to those obtained in wild-type and the complemented strain.

Figure S9

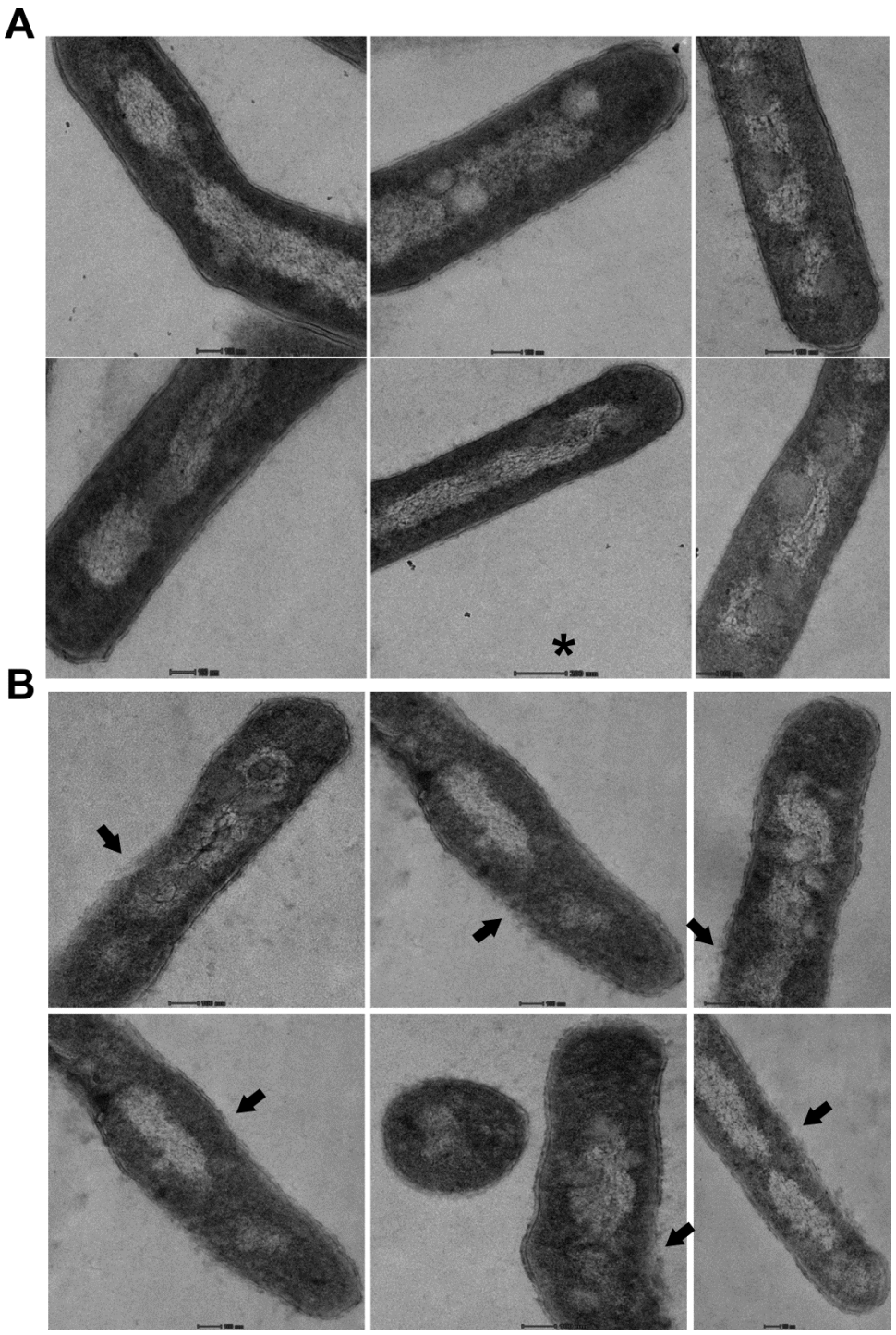

Figure S9. Transmission electron microscopy-based ultrastructural analysis of *M. smegmatis*. Multiple TEM micrographs of WT (A) and Δ*atpD* (B) are shown. The suggested

differences in the cell envelope of Δ*atpD* are marked with arrowhead in panel B. The bar at the bottom of each panel represents the 100 nm scale; panel marked with '*' has 200 nm scale bar.

Figure S10

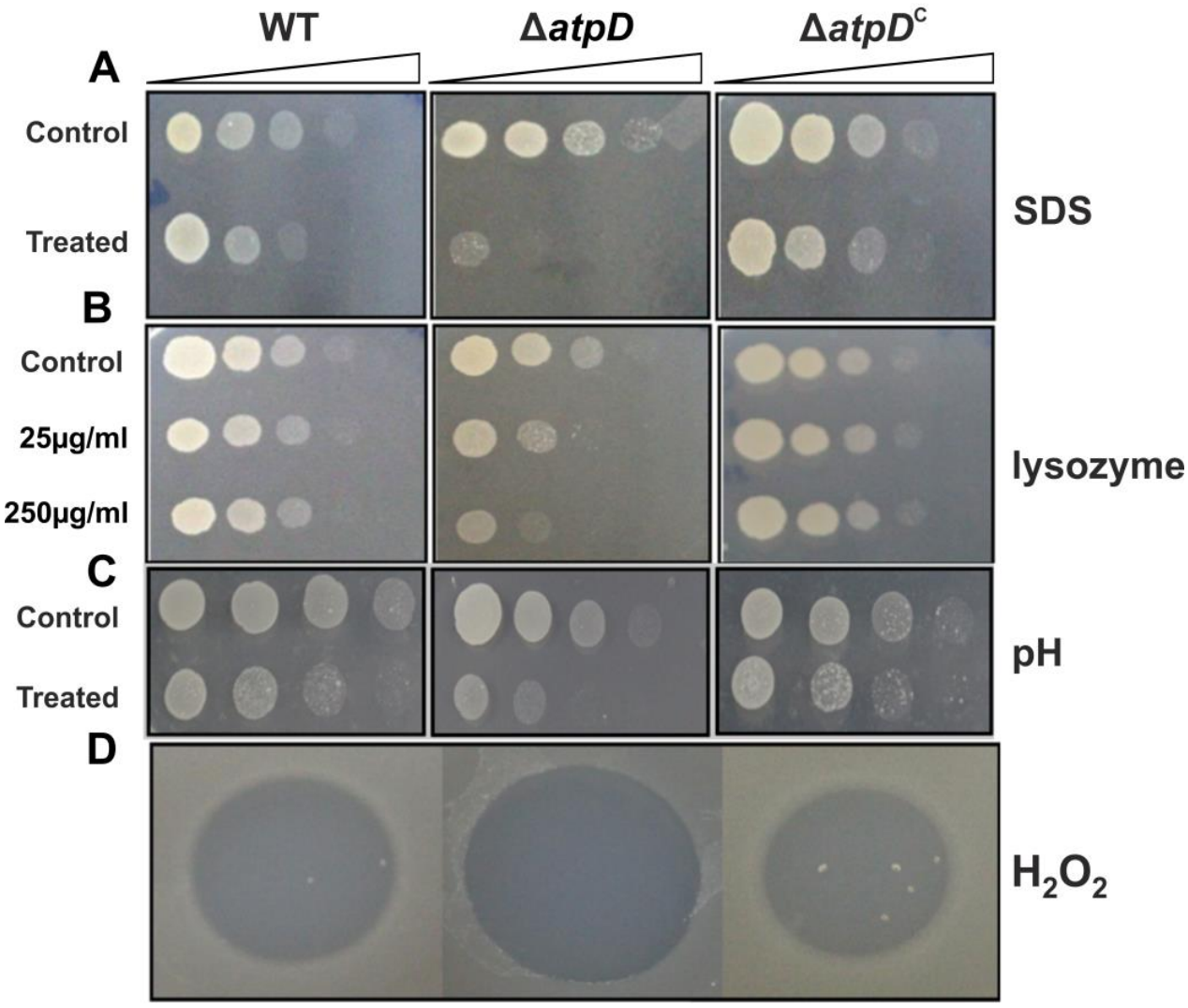

Figure S10. *M. smegmatis* Δ*atpD* is more susceptible to SDS, lysozyme, acidic pH, and peroxide as compared to WT and Δ*atpD*^{C}. Panels show MB7H9-agar plate images of the bacteria spotted after treatment with 0.1% SDS (A), 25 and 250 μg/ml lysozyme (B), pH 5.5 (C), and 5 mM H_2O_2 (D), for a period of 24 h. In panels A-C, four dilutions (marked as triangle) were spotted. In all the panels, Δ*atpD* is found to be more susceptible to the given stress as compared with the WT and the complemented strain. Experiments were repeated multiple times; only one representative image is shown in each panel.

Figure S11

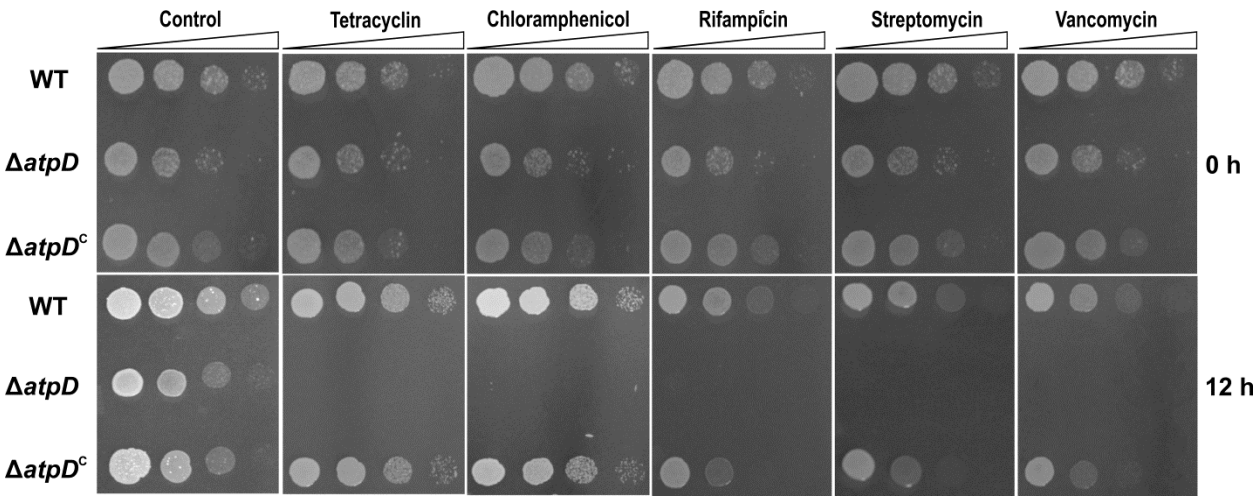

Figure S11. *M. smegmatis* Δ*atpD* is highly susceptible to antibiotic-mediated killing. Panels show the MB7H9-agar plate images of the bacteria spotted after treatment with various antibiotics such as 3 μg/ml tetracycline, 32 μg/ml chloramphenicol, 40 μg/ml rifampicin, 4 μg/ml streptomycin, and 5 μg/ml vancomycin, for the indicated time point (in h) and dilutions (shown as triangle mentioned above each panel). Control is devoid of any antibiotic. Δ*atpD* is found to be more susceptible to all the antibiotics tested as compared with the other two bacteria. Experiment was repeated multiple times, with only one representative image shown in each case.

Figure S12

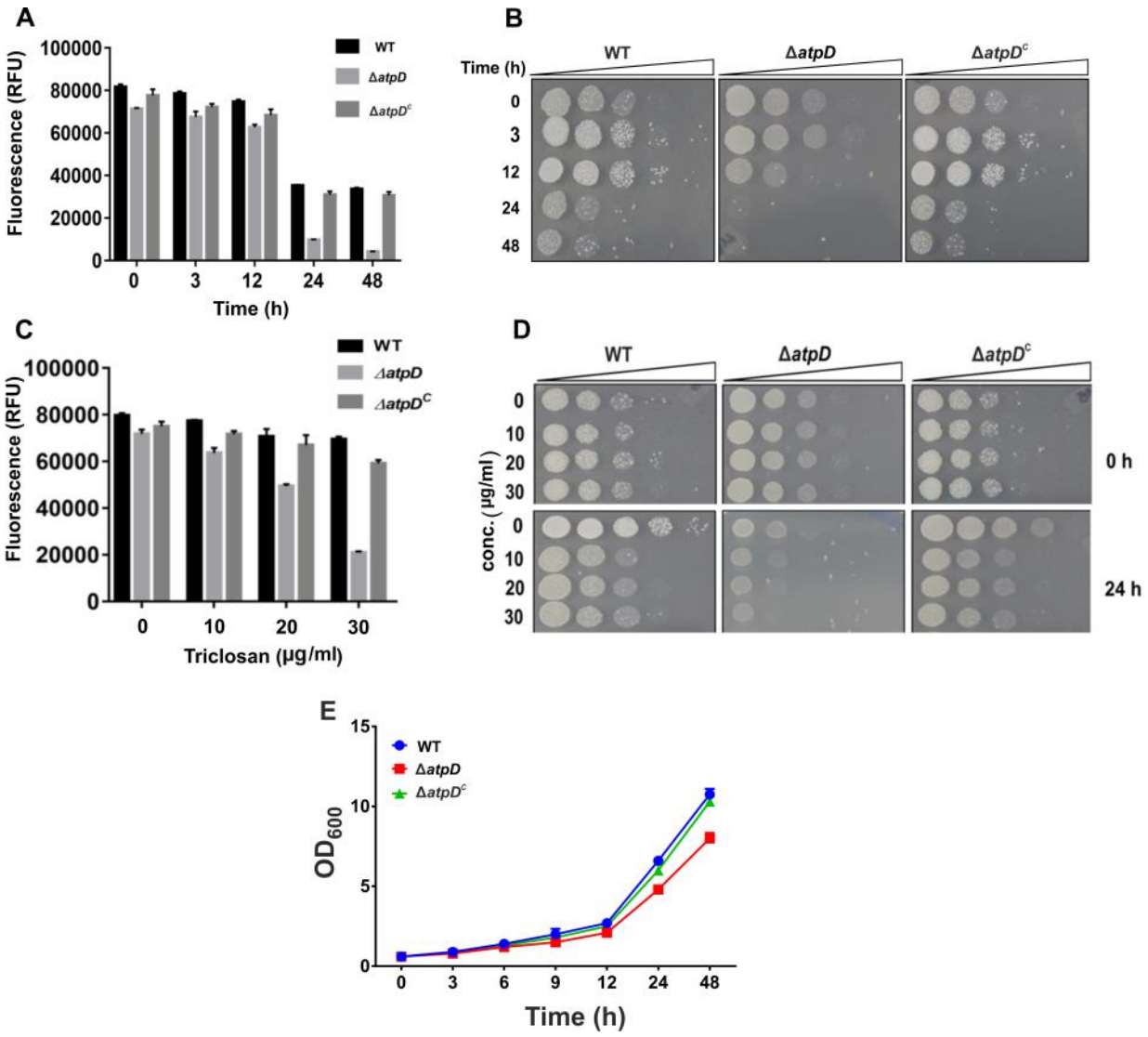

Figure S12. *M. smegmatis* Δ*atpD* is highly susceptible to isoniazid and triclosan. Panel A shows the cell viability data obtained using alamar blue assay in the form of fluorescence upon treatment of bacterium with 20 µg/ml of isoniazid. Antibiotic was added at time 0 and the viability of bacteria was monitored with time for 48 h. While the wild-type (WT) and the complemented strain ($\Delta atpD^C$) show higher fluorescence even after 48 h, knockout cells show less fluorescence. Panel B shows the spot assays of the culture used in panel A and the data

largely corroborate with the alamarBlue assay. Several dilutions of the cultures (shown as triangles) were spotted on MB7H9-agar plate. Similarly, panel C shows the cell viability data obtained using alamarBlue assay upon treatment of bacterium with various concentrations of triclosan ranging from 0 to 30 μg/ml. Antibiotic was added at time 0 and the viability of bacteria was monitored at time 0 and after 24 h. While the wild-type (WT) and the complemented strain ($\Delta atpD^{C}$) show higher fluorescence even at 30 μg/ml triclosan after 24 h, knockout cells show significantly less fluorescence at this concentration. Panel D shows the spot assays of the culture used in panel C at time 0 and after 24 h, and the data largely corroborate with the alamarBlue assay. Several dilutions of the cultures (shown as triangles) were spotted on MB7H9-agar plate. Panel E represents the growth profile of untreated wild-type (WT), Δ*atpD*, and $\Delta atpD^{C}$ strains for an easy comparison with the antibiotic-treated culture (see Fig. 6A and B). In panels A, C, and E, the data represent an average of at least three independent experiments with standard deviation. In both panels B and D, only one representative image in each case is shown.

Figure S13

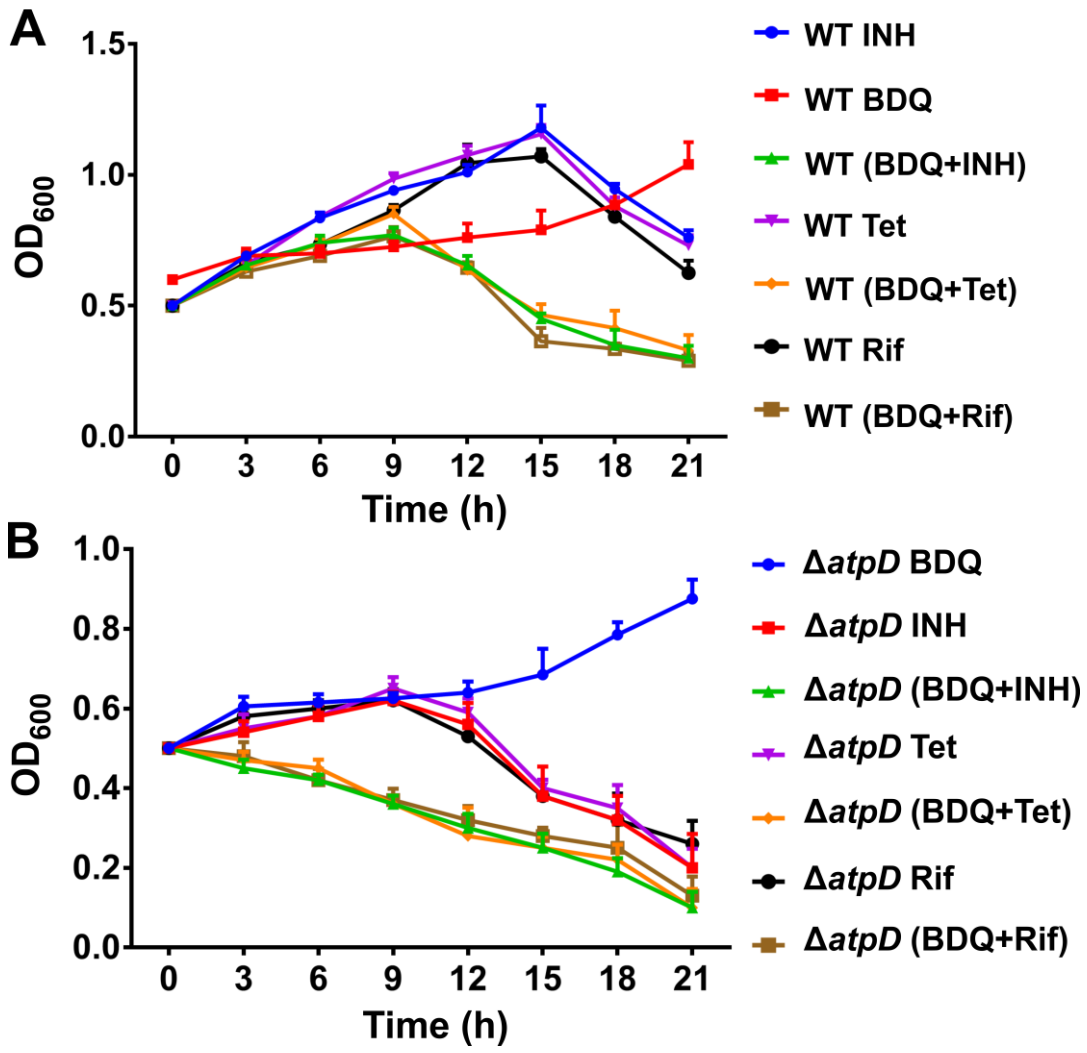

Figure S13. Bedaquiline sensitizes *M. smegmatis* to other antibiotics. Panels A and B represent the wild-type (WT) and the Δ*atpD* strain, respectively, to which BDQ was added at sub-lethal concentration of 0.0001 µg/ml along with other antibiotics, as specified (INH, isoniazid; Tet, tetracycline; Rif, rifampicin). Addition of BDQ in the medium is found to enhance the killing of bacterium as compared to the effect of the respective antibiotic alone in culture medium. The experiments in each case were repeated multiple times. The plots show the average data of at least three independent experiments with standard deviation depicted as error bars.

Figure S14

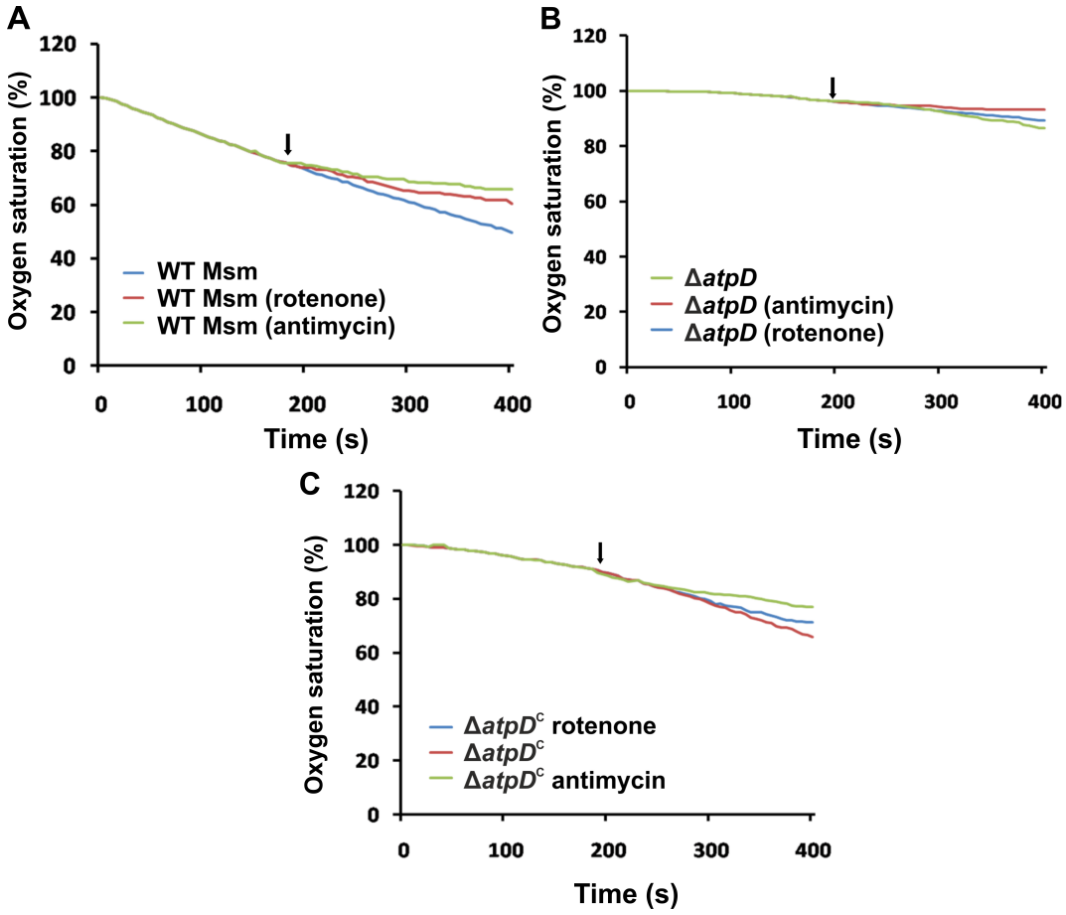

Figure S14. Oxygen consumption by the bacterium in the presence of electron transport chain inhibitors. The panels show the change in dissolved oxygen (oxygen saturation) that occurs in each case with time; at the start of the experiment, this value is considered as 100%.Oxygen consumption in all the three bacteria *viz*. WT (panel A), Δ*atpD* (panel B), and Δ*atpD*^{C} (panel C) is presented as reduction in the oxygen saturation, which is observed as a downward slope. The arrow in each panel indicates the addition of the ETC inhibitor (rotenone or antimycin) at a final concentration of 0.5µM. The data are representative of three independent experiments with standard deviation. The experiments were repeated at least thrice in each case; only the representative data are shown.

Figure S15

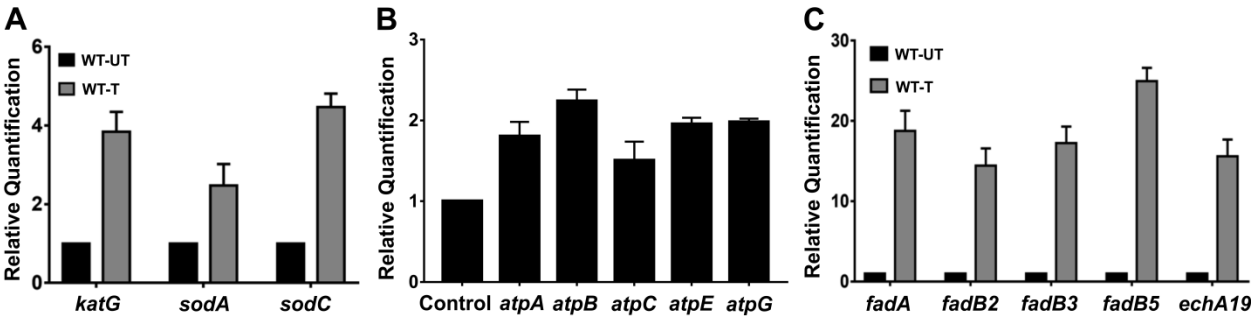

Figure S15. RT-qPCR-based relative quantification of the expression levels of oxidative stress and metabolic pathway genes in bedaquiline-treated WT *M. smegmatis*. Expression analyses of various genes involved in antioxidant defence system genes *katG*, *sodA*, and *sodC* (Panel A), ATP synthase operon genes *atpA*, *B*, *C*, *E*, and *G* (Panel B), and β-oxidation pathway genes *fadA*, *fadB2*, *fadB3*, *fadB5*, and *echA19* (Panel C), as assessed by RT-qPCR are shown. In all the panels, transcript level in the BDQ-treated *M. smegmatis* wild-type (WT-T) is compared with the untreated (WT-UT) strain, which is used as control and is considered as 1; in panel B, the control represents the untreated sample, whereas all others are BDQ-treated. In each graph, the data presented are an average of at least three independent experiments with error bars denoting standard deviation.

SUPPLEMENTAL TABLES

Table S1. List of oligonucleotides used in this study. Oligos and their sequences used to generate and subsequent confirmation of *atpD* knock-out and in the RT-qPCR experiments are presented.

Oligos used for the construction and subsequent confirmation of gene knockout	
Oligo	**Sequence (5'-3')**
atpD_up_for	GGGCTACTTCAGCTTCCGG
atpD_up_rev	CTCGCCCTTGCTGGTCTTTTCTGCAGTAGCAGTCATTC
atpD_down_for	GAGCTGTACAAGTAGTTGCCATGTCCTTGAGCGTC
atpD_down_rev	CGATCACACCGTGCCGCCAC
atpD_hygup_rev	CGTACATCACCACGGTCTTTTCTGCAGTAGCAGTC
atpD_hygdown_frw	GCCCCCCGGATCTTGCCATGTCCTTGAGCGTCC
Hyg_for_atpD	GCAGAAAAGACCGTGGTGATGTACGTGGCGAAC
Hyg_rev_atpD	CAAGGACATGGCAAGATCCGGGGGGCGTCAGG
ko_frw	GACCAACGTCATCTCGATCACCGACGGCCAG
ko_rev	GTTGCTGTGGGGGGCGCGAAAAACAGCGTC

Oligos used in RT-qPCR experiments		
Oligo	**Sequence (5'-3')**	**Gene**
sodA_RT_frw	GTGACCACGCGGCCATCTTCCTG	*sodA*
sodA_RT_rev	CTGTGCCTGGAACTTGTCGAACG	

sodC_RT_frw	AAGTGCGAGGCGAACTCCGTCG	*sodC*
sodC_RT_rev	CGTGAACGCATCGGTGGTG	
katG_RT_frw	GTGGGCCGACCTGATCGTGTATG	*katG*
katG_RT_Rev	GGTTCTCCAGGTCACGCTCAC	
4891_RT_Frw	CAAGGACTTCACGTTCGTGTGC	*ahpC*
4891_RT_Rev	GTCGGCGACACCGTCGGCGTTG	
4890_RT_Frw	GATCTCGGAGGACGCGCTCGAC	*ahpD*
4890_RT_Rev	CACCGGGGTTGCCGATGATG	
5241_RT_frw	GGGACAAGGTGTTCGGCAACCTG	*dosS*
5241_RT_rev	GCAGTTGGGTGCCGATGTCG	
5244_RT_frw	GTCGCGGTGCTCGACGTGC	*dosR*
5244_RT_rev	GATGGCCTGCGCGAGTTCCATG	
fadA_RT_frw	GATTCGAGTGTCGAGAAGCTCG	*fadA*
fadA_RT_rev	GTTTCGGCGTCGACGAAGTAC	
fadB2_RT_frw	GATCATGAAGATCGCGGCGTC	*fadB2*
fadB2_RT_rev	GAAGTTCACCACGAAGCCGGAC	
fadB3_RT_frw	GTCGACGTCAAGAAGGAAGTGC	*fadB3*
fadB3_RT_rev	GAGGTCCTTGACGGAGTCGATC	
fadB5_RT_frw	GTGTGGTCGAACGTCGTGATG	*fadB5*
fadB5_RT_rev	GTCGCGGCAGATTCCGAGTTTTTC	
echA19_RT_frw	GTTACTTCTGCTCGGGCATG	*echA19*
echA19_RT_rev	CTCGGAGATCCCGAACTTG	

4938_RT_frw	CTGCAGACCGGCATCAAGGCCATC	*atpA*
4938_RT_rev	CTGGCCGATGGCGACGTAGACG	
4942_RT_frw	ACTGCCGTCACCGCCGTGATCG	*atpB*
4942_RT_rev	GATCAGGATGAACACGAAGATCGTC	
4935_RT_frw	ACCGCCGGTGAGATCGGCATCC	*atpC*
4935_RT_rev	GTCGATCTCGGACTCGAATTGTGC	
4941_RT_frw	GGATCTCGATCCCAACGCCATC	*atpE*
4941_RT_rev	ACGCGGCTTCCACCAGACCGAC	
4937_RT_frw	CTGTGCGGTGCCTACAACGCCAAC	*atpG*
4937_RT_rev	GAAGCTGAAGTAGCCCAACGCCTTAC	
Atpsyn_beta_RT_for	CAAGGACTTCGAGCACTGGTC	*atpD*
Atpsyn_beta_RT_rev	GATACGGTTGATCATCTCCTGGATC	
0255_RT_frw	CGGAGTACGTCGTCGTCTCGATG	*pck*
0255_RT_rev	GTATCCCGAGCCGAAGCTCCAG	
Icl_RT_for	CGAGCAGATCCAGCACGACTGG	*icl*
Icl_RT_rev	GTCCATGTCGTGCAGCTGCTCC	
msrt_frw	GTACAACAAGATCCGTGGCGACAAG	*glcB*
msrt_rev	GTGCGCCGTCGTCGATTTTCAG	
rpoB_RT_for	TCGATGTCACTGTCCTTCTCGGATC	*rpoB*
rpoB_RT_rev	GACCGTCTGGCTCTTGATCTC	
BlaI_RT_Frw	GCGAAGAAGAACCTCGTCGTGCAG	*MSMEG_3630*
BlaI_RT_Rev	CTGCTTGCTCTCGAGTTCCTCG	

Table S2. Values of NAD^+ and NADH obtained in WT, Δ*atpD*, and Δ*atpD*^{C} strains. Given values for the nucleotides are in pmol. NADH/NAD^+ depicts the ratio of the two nucleotides.

Nucleotide	pMVAcet WT	pMVAcet Δ*atpD*	pMVAcet Δ*atpD*^{C}
NADH (in pmol)	31.8	43.6	31.6
NAD^+ (in pmol)	35.1	33.1	32.0
NADH/NAD^+	0.905	1.31	0.98

Table S3. Changes in the lipid composition in WT, Δ*atpD* and Δ*atpD*^{C} strain. Three lipids GPL, Polar, and Apolar are presented with their corresponding one representative ESI peak. Peak intensity is given as high or low depicting how it is observed in the spectrum.

Lipid	**ESI peak (m/z)**	**Peak Intensity**		
		pMVAcet WT	**pMVAcet Δ*atpD***	**pMVAcet Δ*atpD*^{C}**
GPL	701.48	High	Low	High
Polar	507.60	High	Low	High
Apolar	651.20	Low	High	Low